ACS Sustainable Chemistry & Engineering

Research Article

Cite This: ACS Sustainable Chem. Eng. 2019, 7, 6769−6781

pubs.acs.org/journal/ascecg

Co-liquefaction of Macroalgae with Common Marine Plastic Pollutants

Sofia Raikova,[†] Timothy D. J. Knowles,[‡] Michael J. Allen,*[,§,∥] and Christopher J. Chuck*[,⊥]

[†]Centre for Doctoral Training in Sustainable Chemical Technologies, Department of Chemical Engineering, University of Bath, Claverton Down, Bath BA2 7AY, United Kingdom

[‡]Bristol Radiocarbon Accelerator Mass Spectrometer, University of Bristol, 43 Woodland Road, Bristol BS8 1UU, United Kingdom

[§]Plymouth Marine Laboratory (PML), Prospect Place, The Hoe, Plymouth PL1 3DH, United Kingdom

[∥]College of Life and Environmental Sciences, University of Exeter, Stocker Road, Exeter, EX4 4QD, United Kingdom

[⊥]Department of Chemical Engineering, University of Bath, Claverton Down, Bath BA2 7AY, United Kingdom

Supporting Information

ABSTRACT: Macroalgal blooms are environmentally problematic and costly to remediate, but they also represent a vast untapped resource for the production of renewable chemicals and fuels. The responsible exploitation of such marine resources will become increasingly prominent in the transition away from the crude oil economy that currently dominates global productivity. However, crude oil-derived plastic pollution is now a ubiquitous presence in the marine environment, which hampers the effective conversion of marine feedstocks. If the full potential of macroalgae is to be realized, any large-scale industrial process will need to accommodate the presence of this plastic. This study, for the first time, aimed to assess the effect of several common marine plastic pollutants on the hydrothermal liquefaction (HTL) of four UK macroalgae species and determine the impact on the major HTL products and biocrude oil quality. Co-liquefaction of polyethylene and polypropylene with *L. digitata*, *U. lactuca*, *F. serratus*, and *S. muticum* led to modest synergistic effects for plastic conversion. Under hydrothermal conditions, polyethylene underwent fragmentation to olefinic species, as well as oxidative depolymerization to form ketones. Modest synergistic effects on biocrude production were also observed for polypropylene, which depolymerized more readily in the presence of biomass to form gaseous propylene as well as oil-phase products. In both cases, the presence of plastics increased total biocrude carbon content, decreased nitrogen, and boosted higher heating value (HHV), constituting an overall improvement in biocrude fuel properties. Alternatively, nylon-6, typically originating from fisheries debris, depolymerized almost entirely under HTL conditions to form caprolactam, which partitioned mainly to the aqueous phase. While this is not favorable for biocrude production, the reclamation of marine nylon debris for hydrothermal processing to monomers may present a promising revenue stream in future biorefineries. The results demonstrate that plastic contaminants may well represent an opportunity, rather than a threat, to the successful development of an HTL macroalgal biorefinery.

KEYWORDS: *Plastic, HTL, Macroalgae, Seaweed, Biofuel, Environmental remediation*

INTRODUCTION

There is a pressing need to decarbonize global energy production systems, and biofuels compatible with current refinery and transportation infrastructure are a vital component of the transition. Macroalgae represent a particularly promising and under-exploited feedstock for advanced biofuel production, with substantially higher growth rates and photosynthetic efficiencies than terrestrial crops[1] and, unlike microalgae, mature cultivation and harvesting technologies. Hydrothermal liquefaction (HTL) is a thermochemical processing method, ideally suited to high-moisture marine biomass, and macroalgal HTL has attracted increasing attention in recent years.[2,3]

A key advantage of macroalgae over microalgae as a large-scale biofuel feedstock is the ability to cultivate and harvest in situ, in marine environments. Macroalgae take up dissolved nutrients directly from seawater, and thus do not require additional fertilizer input or artificial illumination (as is the case for microalgal cultivation). Cultivation of macroalgae is well-developed in parts of Asia,[4] but cultivation projects are also being established across Europe[5−7] and East Africa.[8]

Received: November 20, 2018
Revised: March 8, 2019
Published: March 11, 2019

Macroalgal cultivation is also utilized to great effect for remediation of waters contaminated by terrestrial agricultural runoff or wastewater from fish aquaculture.[9−14] However, one of the most concerning forms of water pollution at the present moment is marine plastics, which have attracted a significant amount of research interest,[15] as well as increasing media attention, in recent years. The removal of "contaminating" macroplastics following harvesting is a standard feature of macroalgae preprocessing procedures.[16,17] However, to develop a practical and effective industrial process based on macroalgae (whether cultivated or from harvested natural stocks), any biorefinery-based process will need to accommodate both the natural variation in biomass composition and variations in plastic abundance and composition.

Marine plastics originate primarily from single-use packaging,[15] such as plastic drink bottles and polyethylene (PE) bags, as well as a smaller contribution from maritime debris, such as nylon from fishery activities.[18] Recent studies estimate that a minimum of 5.25 trillion plastic particles are afloat in the ocean, weighing almost 300 000 tonnes,[19] although this figure excludes debris on the seafloor, as well as litter washed up on beaches. Marine litter is degraded by physical and chemical means to microplastics,[20] which are ingested by marine biota, making their way up the food chain to human consumption,[18,21] and both micro- and macroplastics have now become ubiquitous at all strata of the ocean, including the deep ocean floor.[22] As a result, harvested crops of marine macroalgae are likely to be associated with both plastic litter and microplastics, which adsorb onto macroalgal surfaces,[21] in increasing quantities. Larger debris could potentially be removed manually during biomass preparation for processing, but residual microplastics can remain even after washing,[21] meaning that macroalgal fuel feedstocks are always likely to contain some level of plastic. However, this can potentially be used to an advantage, coupling fuel production with simultaneous marine plastic remediation.

Coprocessing of lignocellulose and microalgae with plastic wastes, including co-pyrolysis[23,24] and co-liquefaction,[25−27] has been investigated previously. Synergistic effects (SEs) between plastic and microalgae on yields of biocrude from liquefaction have been observed. The presence of highly reactive biomass decomposition products have been shown to lower the thermal stability of PE and accelerate its thermal degradation at lower temperatures; PE, in turn, can act as a hydrogen source in biomass liquefaction.[27,28] Co-liquefaction of PE with Spirulina was found to decrease the oxygen content of the biocrude products,[27] while we have previously demonstrated that co-liquefaction of Vietnamese *Ulva intestinalis* with PE gave biocrudes with decreased nitrogen levels and increased higher heating value (HHV),[28] an overall improvement in fuel properties. The presence of plastics was also found to promote the conversion of biomass to biocrude.

The aim of this investigation was to assess co-hydrothermal liquefaction of a wider range of UK macroalgae species with a range of plastics commonly found in marine environments (PE, polypropylene (PP), and nylon-6 (NY)) in order to model the effect of plastic contaminants on macroalgal biocrude production within a marine biorefinery context. Biomass feedstock species were selected with the overarching aim of developing a future biorefinery for the simultaneous production of biofuels and remediation of marine plastic pollution. *Laminaria digitata*, cultivated at large scales worldwide, with mature and well-developed cultivation and harvesting technologies, was therefore of particular interest, among other common UK species. The effect of plastics on the yields and compositions of the product phases was examined, and potential valorization routes for each product phase were assessed.

EXPERIMENTAL SECTION

Materials and Apparatus. Fresh macroalgal biomass samples were collected from Saltern Cove, Paignton, Devon. Contaminating macroplastics and other debris were removed by hand prior to snap freezing in liquid nitrogen and storage at −80 °C. Prior to analysis, all biomass samples were freeze-dried and milled to ca. 500 μm diameter. Freeze-dried samples were stored at ambient conditions.

Granulated (approximately 500 μm) PE and PP were obtained from Sigma-Aldrich. Pelletized NY was obtained from Alfa Aesar; the particle size was reduced to <500 μm using a commercial food processor. Plastics were stored at ambient conditions prior to use.

Unstirred bomb-type batch reactors were fabricated according to literature precedent using stainless steel Swagelok tube fittings.[29−31] The reactor body consisted of a length of stainless steel tubing capped at one end and connected at the other to a pressure gauge, thermocouple, needle valve, and relief valve. The total internal volume of the reactors was ca. 50 cm^3. A reactor schematic is available in the Supporting Information.

Procedures. Reaction procedures have been reported previously.[31] In a typical reaction, the reactor was loaded with 3 g of material (biomass mixed with plastics, with biomass:plastic ratios of 100:0, 90:10, 75:25, 50:50, and 0:100; a full experimental table is provided, Table 1) and 15 cm^3 of freshly deionized water, and heated within a vertical tubular furnace until the specified reaction temperature (340 °C ± 3 °C) was reached. The reactor was subsequently removed from the furnace and allowed to cool to room temperature. The overall heating time was 12−27 min. Pressure within the reactors was generated in situ by the expansion of water and volatiles and typically reached 150 bar.

After being cooled, gaseous products were released via the needle valve into an inverted, water-filled measuring cylinder to measure the gaseous fraction volume. Gas phase yields were calculated using the ideal gas law, approximating the gas phase as 100% CO_2, assuming an approximate molecular weight of 44 g mol^{-1} and a volume of 24.6 dm^3 mol^{-1} gas phase at 25 °C. The yield of gaseous product was determined using the following equation

$$\text{yield}_{\text{gas}} = \frac{V_{\text{gas}} \times 1.789 \times 10^{-3}}{m_{\text{dry biomass}} + m_{\text{plastic}}} \times 100\% \quad (1)$$

Following this, the aqueous phase was decanted from the reactor contents and filtered through a Fisher qualitative filter paper predried overnight at 60 °C. The product yield in the water phase was determined by leaving a 2.5 g aliquot to dry in a 60 °C oven overnight, and scaling the residue yield to the total aqueous phase mass. The aqueous phase residue yield was determined using the following equation

$$\text{yield}_{\text{AP residue}} = \frac{m_{\text{AP residue}}}{m_{\text{dry biomass}} + m_{\text{plastic}}} \times 100\% \quad (2)$$

To separate the remaining biocrude oil and char phase, the reactor was washed repeatedly using chloroform until the solvent ran clear and filtered through the same filter paper used to separate the aqueous phase (after being dried for a minimum of 1 h). The filter paper and collected char were washed thoroughly with chloroform to remove all remaining biocrude. The filtrate was collected, the solvent was removed in vacuo (40 °C, 72 mbar) until no further solvent evaporation was observed visually, and biocrude samples were left to stand in septum-sealed vials venting to the atmosphere via a needle for a further 12 h to remove residual solvent. The biocrude yield was determined using the following equation

DOI: 10.1021/acssuschemeng.8b06031
ACS Sustainable Chem. Eng. 2019, 7, 6769−6781

Table 1. Full Experimental Table

	macroalgae species	plastic	biomass:plastic ratio	temperature (°C)	pressure (bar)	heating rate (°C min^{-1})	heating time (min)
1	*L. digitata*		100:0	342.5 ± 2.5	165 ± 15	25 ± 5	12 ± 1.5
2	*L. digitata*	PE	90:10	342.5 ± 2.5	165 ± 15	25 ± 5	12 ± 1.5
3	*L. digitata*	PE	75:25	342.5 ± 2.5	165 ± 15	25 ± 5	12 ± 1.5
4	*L. digitata*	PE	50:50	342.5 ± 2.5	165 ± 15	25 ± 5	12 ± 1.5
5	*L. digitata*	PP	90:10	342.5 ± 2.5	165 ± 15	25 ± 5	12 ± 1.5
6	*L. digitata*	PP	75:25	342.5 ± 2.5	165 ± 15	25 ± 5	12 ± 1.5
7	*L. digitata*	NY	90:10	342.5 ± 2.5	165 ± 15	25 ± 5	12 ± 1.5
8	*L. digitata*	NY	75:25	342.5 ± 2.5	165 ± 15	25 ± 5	12 ± 1.5
9	*L. digitata*		100:0	342.5 ± 2.5	165 ± 15	11.5 ± 0.5	27 ± 3
10	*L. digitata*	PE	90:10	342.5 ± 2.5	165 ± 15	11.5 ± 0.5	27 ± 3
11	*L. digitata*	PE	75:25	342.5 ± 2.5	165 ± 15	11.5 ± 0.5	27 ± 3
12	*F. serratus*		100:0	342.5 ± 2.5	165 ± 15	25 ± 5	12 ± 1.5
13	*F. serratus*	PE	75:25	342.5 ± 2.5	165 ± 15	25 ± 5	12 ± 1.5
14	*F. serratus*	PE	50:50	342.5 ± 2.5	165 ± 15	25 ± 5	12 ± 1.5
15	*F. serratus*	PP	90:10	342.5 ± 2.5	165 ± 15	25 ± 5	12 ± 1.5
16	*F. serratus*	PP	75:25	342.5 ± 2.5	165 ± 15	25 ± 5	12 ± 1.5
17	*F. serratus*	NY	90:10	342.5 ± 2.5	165 ± 15	25 ± 5	12 ± 1.5
18	*F. serratus*	NY	75:25	342.5 ± 2.5	165 ± 15	25 ± 5	12 ± 1.5
19	*S. muticum*		100:0	342.5 ± 2.5	165 ± 15	25 ± 5	12 ± 1.5
20	*S. muticum*	PE	75:25	342.5 ± 2.5	165 ± 15	25 ± 5	12 ± 1.5
21	*S. muticum*	PE	50:50	342.5 ± 2.5	165 ± 15	25 ± 5	12 ± 1.5
22	*S. muticum*	PP	90:10	342.5 ± 2.5	165 ± 15	25 ± 5	12 ± 1.5
23	*S. muticum*	PP	75:25	342.5 ± 2.5	165 ± 15	25 ± 5	12 ± 1.5
24	*S. muticum*	NY	90:10	342.5 ± 2.5	165 ± 15	25 ± 5	12 ± 1.5
25	*S. muticum*	NY	75:25	342.5 ± 2.5	165 ± 15	25 ± 5	12 ± 1.5
26	*U. lactuca*		100:0	342.5 ± 2.5	165 ± 15	25 ± 5	12 ± 1.5
27	*U. lactuca*	PE	75:25	342.5 ± 2.5	165 ± 15	25 ± 5	12 ± 1.5
28	*U. lactuca*	PE	50:50	342.5 ± 2.5	165 ± 15	25 ± 5	12 ± 1.5
29	*U. lactuca*	PP	90:10	342.5 ± 2.5	165 ± 15	25 ± 5	12 ± 1.5
30	*U. lactuca*	PP	75:25	342.5 ± 2.5	165 ± 15	25 ± 5	12 ± 1.5
31	*U. lactuca*	NY	90:10	342.5 ± 2.5	165 ± 15	25 ± 5	12 ± 1.5
32	*U. lactuca*	NY	75:25	342.5 ± 2.5	165 ± 15	25 ± 5	12 ± 1.5
33		PE	0:100	342.5 ± 2.5	165 ± 15	25 ± 5	12 ± 1.5
34		PP	0:100	342.5 ± 2.5	165 ± 15	25 ± 5	12 ± 1.5
35		NY	0:100	342.5 ± 2.5	165 ± 15	25 ± 5	12 ± 1.5

$$\text{yield}_{\text{biocrude}} = \frac{m_{\text{biocrude}}}{m_{\text{dry biomass}} + m_{\text{plastic}}} \times 100\% \quad (3)$$

The char yield was calculated from the mass of the retentate collected on the filter paper after being dried overnight in an oven at 60 °C. The solid yield was determined using the following equation

$$\text{yield}_{\text{solid}} = \frac{m_{\text{solid}}}{m_{\text{dry biomass}} + m_{\text{plastic}}} \times 100\% \quad (4)$$

Inevitable material losses occurred during workup, predominantly through evaporation of light organics from the aqueous and biocrude phases during filtration and solvent removal. The shortfall in the mass balance has thus been designated as "volatiles".

Characterization. Biomass ash was quantified by heating a 500 mg sample of biomass in a Carbolite CWF 11 muffle furnace at 550 °C for 5 h. The mass remaining at the end of the experiment was taken to be the ash.

For macroalgal biomass, biocrude, and char, elemental (CHN) analysis was carried out externally at London Metropolitan University on a Carlo Erba Flash 2000 Elemental Analyzer to determine CHN content. Elemental analyses were carried out at least in duplicate for each sample, and average values are reported. HHV was calculated from elemental composition according to literature precedent.[32]

The aqueous phase products were analyzed for total carbon (TC) and total nitrogen content (TN) using a Shimadzu TOC-L TOC analyzer fitted with a TNM-L total nitrogen analyzer unit and an ASI-L autosampler.

Thermogravimetric analyses (TGA) of HTL solid phases were conducted using a Setaram TG-92. Samples were heated from ambient temperature to 1000 °C at a rate of 20 °C min^{-1} under an air atmosphere.

FTIR spectra were obtained on a Thermo Scientific Nicolet iS5 FTIR spectrometer. All samples were analyzed in the wavenumber range of 4000−500 cm^{-1}.

GC−MS of biocrudes was carried out using an Agilent 7890A gas chromatograph fitted with an Agilent HP5-MS capillary column (30 m × 250 μm × 0.25 μm) and an Agilent 5975C MS detector. Helium (1.2 mL min^{-1}) was used as the carrier gas. Samples were injected (10:1 split injection) at 50 °C, held for 1 min, ramped to 290 °C at a rate of 7.5 °C min^{-1}, and held for 3 min at 290 °C. Tentative identification of the compounds was performed using the NIST mass spectral database.

Gas phases were analyzed using an Agilent 7890A gas chromatograph fitted with an Agilent HP5-MS capillary column (30 m × 250 μm × 0.25 μm), an FID detector, and an Agilent 5975C MSD detector. Helium (1.2 mL min^{-1}) was used as the carrier gas. Gas samples were injected directly onto the column at 40 °C, held for 7 min, then ramped to 150 °C at 20 °C min^{-1}, ramped to 250 °C at 15 °C min^{-1}, and held for 6 min at 250 °C. Identification of compounds was performed using the NIST mass spectral database.

For radiocarbon analyses by accelerator mass spectrometry (AMS), samples were combusted and graphitized with an Elementar Vario Isotope Select elemental analyzer interfaced to an IonPlus AGE3 graphitization system,[33] and radiocarbon determinations were

DOI: 10.1021/acssuschemeng.8b06031
ACS Sustainable Chem. Eng. 2019, 7, 6769−6781

performed using the BRIS-MICADAS AMS. Data reduction was performed using the software package BATS.[34]

In order to determine experimental error and test the repeatability of experimental results, three repeat HTL runs of *L. digitata* were carried out to determine the standard deviation in mass balances. Uncertainty in mass yields was as follows: standard deviation of 3.4% for the gas phase, 1.8% for the aqueous phase, 2.1% for the biocrude, and 1.8% for the char. All elemental analyses (CHN) were carried out in duplicate, and average values were used.

RESULTS AND DISCUSSION

HTL Conversion of Common Marine Plastic Contaminants. PE and PP are highly thermally stable polymers. Thermal decomposition of PE in supercritical water has been reported previously,[35,36] but the behavior of PE at subcritical HTL conditions remains largely unexplored, save for co-liquefaction with residual oil.[37]

HTL of pure PE and PP was carried out. However, upon cooling the reactor, the plastics were found to have partially melted and fused into a solid plug, separate from the water layer, with no measurable gas production and no extractable biocrude.

In contrast, liquefaction of NY at HTL temperatures (340 °C) led to the conversion of 6.6% of the polymeric material to chloroform-soluble "biocrude" product and 10.9% to water-soluble material. Polycondensation polymers such as NY are susceptible to thermal degradation, and NY has been shown to depolymerize by hydrolysis at subcritical conditions to form monomeric ϵ-caprolactam via an ϵ-aminocaproic acid intermediate.[38]

Caprolactam is soluble in both aqueous media and chloroform.[39] Correspondingly, analysis by GC−MS revealed substantial levels of caprolactam partitioned between the biocrude and aqueous phases. The presence of 2,4-di-*tert*-butylphenol in the biocrude phase was also detected. 2,4-Di-*tert*-butylphenol is present in plastics as a UV stabilizer and antioxidant but is, alongside other similar phenolics, also widely used as an antioxidant,[40] which may prove advantageous for fuel production from biocrude derived from nylon-containing feeds by improving fuel storage stability.

Conversion of Plastic-Enriched *Laminaria digitata*. *L. digitata* blended with common marine pollutants PE, PP, and NY was processed using HTL conditions previously reported.[41,42] Product yields were calculated on the basis of total feedstock input; product mass balances are presented in Figure 1, plotted against plastic loading (the percentage of plastic in the feedstock on a mass basis). Mass closures ranged from 70 to 99%, in line with those observed in studies conducted by other researchers.[43]

For liquefaction of biomass alone, the largest proportion of the organic material in the feedstocks (25.1%) was recovered in the aqueous phase products. On the addition of PE, a modest increase in biocrude yield was observed for a 10% blend of PE with *L. digitata*, while decreases in overall biocrude production were seen for 25 and 50% blends (biocrude yields of 10.8 and 8.2%, respectively). The majority of the PE was recovered in the solid phase products, with char yields increasing concomitantly with biocrude depletion, up to a maximum solid yield of 55.5% for a 50% PE blend level, although a notable dip in solid phase recovery (26.5% solid at a 25% PE blend level, down from 31.5% at a 10% PE blend) was observed. Aqueous phase product recovery declined steadily (25.1% for pure biomass, down to 14.3% for a 50% PE blend),

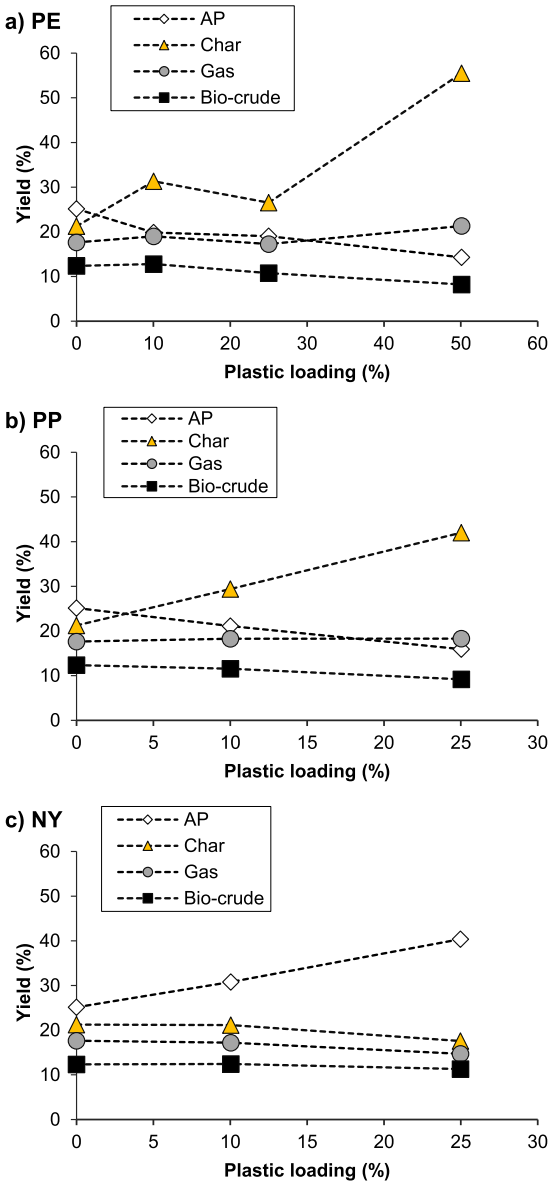

Figure 1. Mass balances of HTL products from liquefaction of *L. digitata* blended with (a) PE, (b) PP, and (c) NY.

while increasing PE blend levels also caused a modest increase in the yield of gas phase products at 10 and 50% blend levels.

A similar pattern of results was observed for PP. Aqueous phase products and biocrude yields declined with increasing PP blend level (down to 9.2% biocrude for a 25% PP blend level), while the gas phase product yield stayed approximately constant. The majority of the plastic-enriched feed was, once again, recovered in the solid phase products (up to a maximum of 42.0% solid yield for a 25% PP blend).

For co-liquefaction with NY, however, increasing the polymer blends caused biocrude production to remain constant at 12.4% upon increasing to a 10% NY blend and decreased to 11.3% for the 25% blend. Gas and solid phase yields declined steadily, while a substantial increase in the aqueous phase product recovery was seen, 40.4% of the total feed partitioned to the aqueous phase for a 25% NY blend level.

For the liquefaction of plastics in the presence of biomass, modest SEs were observed. The extent of SEs between the

DOI: 10.1021/acssuschemeng.8b06031
ACS Sustainable Chem. Eng. 2019, 7, 6769−6781

biomass and plastic reactants was calculated using the equation proposed by Wu et al.[26]

$$\text{Synergistic effect} = Y_{BC} - (X_{macroalgae} \times Y_{macroalgae} + (1 - X_{plastic}) \times Y_{plastic}) \quad (5)$$

where Y_{BC} represents the yield of biocrude in a given experiment, Y_i represents the yield of biocrude from an individual component when processed in isolation, and X_i represents the mass fraction of each component in the reaction mixture. A positive value of SE indicates that a greater yield of biocrude was obtained from the blended feedstock than the linear sum of the yields expected from each of the individual feedstocks, and vice versa.

The degree of SEs for co-liquefaction of *L. digitata* with PE and PP was relatively modest but positive in all cases, with the exception of a 3:1 blend of *L. digitata* with PP (Figure 2).

The presence of any nonpolymeric species, such as residual polymerization catalysts or additives, can affect the resistance of a plastic to thermal degradation. Transition metals, including manganese, can be activated at elevated temperatures and act as a pro-oxidant for PE, generating radicals on the polymer chain, which can then undergo oxidation or chain scission.[44] Ash present in macroalgal biomass can potentially supply metals, which act as pro-oxidants for PE and PP, although it has also been suggested that the presence of organic biomass fragments and radicals can also promote polymer chain scission.[25] Hydrogen transfer from polyolefinic chains can, in turn, stabilize radicals generated by biomass thermal degradation and prevent recondensation to solid char, generating higher oil yields.[25] It is noted that these effects may be temperature-dependent, and SEs may diminish beyond a certain temperature threshold.[25]

Effect of Heating Rate. The heating rate plays a significant role in determining HTL outcomes.[41,45,46] This was investigated using pure *L. digitata* and *L. digitata* blended with PE at a 10% blend level. The reaction temperature remained constant at 340 °C, but heating rates were varied from 11 to 25 °C min^{-1}.

The degree of SEs seen for biocrude production was not the same for the two heating rates, with a positive SE observed for HTL carried out at a heating rate of 25 °C min^{-1}, but negative effects observed for 11 °C min^{-1} (Figure 3). This suggests that for optimal PE conversion under HTL conditions, elevated heating rates are preferred. This is advantageous, as short

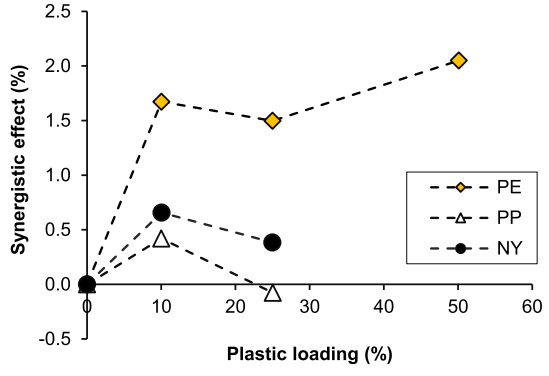

Figure 2. SEs on biocrude yields from liquefaction of *L. digitata* blended with plastics (PE = polyethylene, PP = polypropylene, and NY = nylon-6).

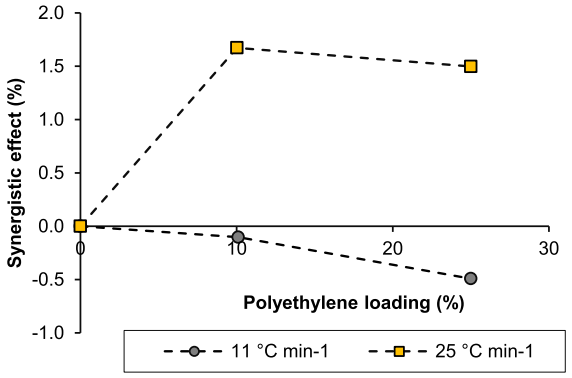

Figure 3. SEs on biocrude production for co-liquefaction of *L. digitata* with PE over two different heating rates.

reaction times and high heating rates are also preferred for the production of biocrude from macroalgal biomass,[41] and it will therefore not be necessary to compromise on heating rates to obtain optimal conversion of both biomass and plastics.

Biocrude Composition. Plastic co-liquefaction had a significant impact on biocrude elemental composition (Figure 4). Co-liquefaction of *L. digitata* with increasing blends of PE led to an increase in both carbon and hydrogen, thereby increasing biocrude HHV (an initial modest increase from 33.5 to 34.2 MJ kg^{-1} on moving from pure *L. digitata* to a 25% PE blend and a more substantial jump to 39.3 MJ kg^{-1} for 50% PE). A corresponding decrease in biocrude nitrogen was also observed. These changes equate to an overall improvement in biocrude fuel properties.

The plastics may be solubilized by the biomass conversion products or, alternatively, thermally degraded into monomeric or oligomeric fragments, which can react with reactive intermediate biomass decomposition products. It has also been proposed that under pyrolytic conditions (i.e., in the absence of H_2O), polyolefins can readily donate hydrogen to biomass radicals.[47] For hydrothermal conditions, D_2O studies have demonstrated that H_2 can be liberated from water and migrate to the biocrude phase products,[35] but polymers may also act as a hydrogen source in hydrothermal coprocessing,[25] potentially contributing to the increase in biocrude hydrogen.

For co-liquefaction with PP, the overall impact on biocrude elemental composition was similar to that observed for PE, although the reduction in nitrogen content was somewhat more modest. For co-liquefaction with nylon, hydrogen levels stayed approximately constant, but a significant depletion in carbon was observed (from 73.7% for pure *L. digitata* to 65.4% for a 25% NY blend), alongside a corresponding depletion in HHV (33.5 to 30.3 MJ kg^{-1}). A substantial increase in nitrogen to 5.4% for the 25% NY blend from 3.4% for a pure *L. digitata* feedstock was also seen. The presence of elevated nitrogen in crude can poison refinery catalysts and lead to elevated NO_x emissions on combustion, and high-nitrogen crudes require extensive hydrotreatment prior to use, so the presence of NY in feedstocks may have detrimental effects on biocrude fuel properties.

FT-IR spectra of biocrudes obtained from liquefaction of pure *L. digitata* and *L. digitata* blends with PE, PP, and NY are presented in Figure 5. Co-liquefaction of *L. digitata* with increasing blends of PE gave rise to increasing intensity in absorbance at 2916 cm^{-1}, attributable to C−H stretching, with an attendant decrease in the broad peak at 3650−3100 cm^{-1}, arising from N−H and O−H stretching in alcohols and

DOI: 10.1021/acssuschemeng.8b06031
ACS Sustainable Chem. Eng. 2019, 7, 6769−6781

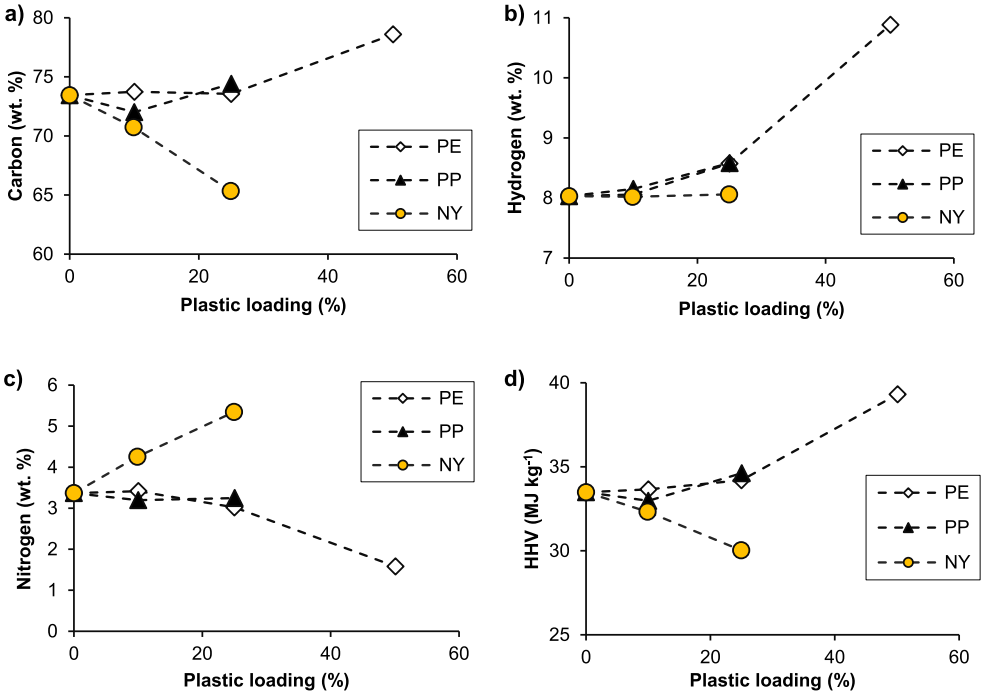

Figure 4. Biocrude compositions produced from the co-liquefaction of *L. digitata* with PE, PP, and NY, where (a) is carbon wt %, (b) hydrogen wt %, (c) nitrogen wt %, and (d) is HHV of the biocrudes.

amines. A sharpening of the C═O ketone stretch at 1700 cm^{-1} was also observed, although overall absorbance decreased. These observations are supported by GC−MS analysis. Similar changes in IR absorbance were observed for biocrudes produced from co-liquefaction with PP, although the differences were somewhat less pronounced. For co-liquefaction with NY, increasing blend levels gave rise to an amide C═O stretch at 1629 cm^{-1} not observed in biocrude obtained from pure *L. digitata* as well as a N−H stretch at 3300 cm^{-1}.

Analysis of the biocrudes by GC−MS allowed for a more in-depth assessment of biocrude composition. Biocrude derived from *L. digitata* alone contained primarily phenolic species, with a contribution from organic acids formed via the depolymerization of lipids. A full compositional breakdown of the volatile fraction of the biocrudes can be found in the Supporting Information. Under HTL conditions, PE was expected to show random bond scission along the chain, resulting in producing a distribution of aliphatic hydrocarbons of varying length,[27] including a substantial contribution from alkenes.[48] Indeed, for co-liquefaction of *L. digitata* with PE, at 10 and 25% blend levels, the emergence of low levels of long-chain aliphatic hydrocarbons ($\geq C_{13}$) was observed. Additionally, the common plasticizer bis(2-ethylhexyl)phthalate was present in biocrudes as well as a substantial contribution from long-chain ketones ($\geq C_{12}$). These were formed in substantially higher quantities when *L. digitata* was processed at a 50% blend level with PE. It is noteworthy that PE processed under analogous HTL conditions in isolation (i.e., without macroalgal cofeedstock) did not produce biocrude oil. An overlay of the GC−MS chromatograms for the biocrudes is presented in Figure 6, with key compounds identified in Table 2.

A significant proportion of the peaks formed only in the presence of PE are long chain ketones. An increase in ketone levels has also been observed by Wu et al. for the co-liquefaction of microalgae and PP.[26] HTL reaction mechanisms are complex and not fully understood, due to the occurrence of hundreds of simultaneous reactions. Under hydrothermal conditions, radical species are formed via C−C scission;[49] the emergence of long-chain ketones in the biocrude is, therefore, speculated to originate from PE via a radical oxidation mechanism. Moriya et al. have suggested that alcoholic intermediates are formed initially and subsequently converted to their corresponding ketones,[35] but the conspicuous absence of long-chain alcohols in the final products suggests that the reaction may instead proceed via an unstable hydroperoxide intermediate.[50] Long-chain alcohols are stable and slower to oxidize, and their presence has been found to inhibit the oxidation of long-chain paraffins.[50] The mechanism is initiated via the abstraction of a proton from a CH_2 adjacent to a terminal methyl group by an alkyl radical. This is followed by the reaction of the resulting PE radical with dissolved O_2, reaction with a hydrogen radical to generate an −OOH group, and finally, dehydration to generate a ketone end group. A summary of the proposed mechanism is presented in the Supporting Information.

The presence of metals in the biomass ash may also play a catalytic role in ketone formation. Hydroperoxide conversion to ketones has also been shown to be catalyzed by copper and iron stearates,[50] and these species could feasibly arise in situ from degradation of biomass lipids to fatty acids in the presence of cuprous and ferric species in biomass ash. Co-liquefaction of biomass with NY resulted in the emergence of a large peak attributable to caprolactam (Figure 7). NY depolymerizes in water at temperatures as low as 100 °C to generate ϵ-aminocaproic acid and, subsequently, undergoes cyclodehydration to ϵ-caprolactam (as well as further degradation to smaller molecules).[38,51] The presence of caprolactam in the HTL products may also arise, in part, from residual monomer present in the NY. Correspondingly, total detectable nitrogen in the aqueous phase products was found to increase. Other nitrogen-containing species formed in

DOI: 10.1021/acssuschemeng.8b06031
ACS Sustainable Chem. Eng. 2019, 7, 6769−6781

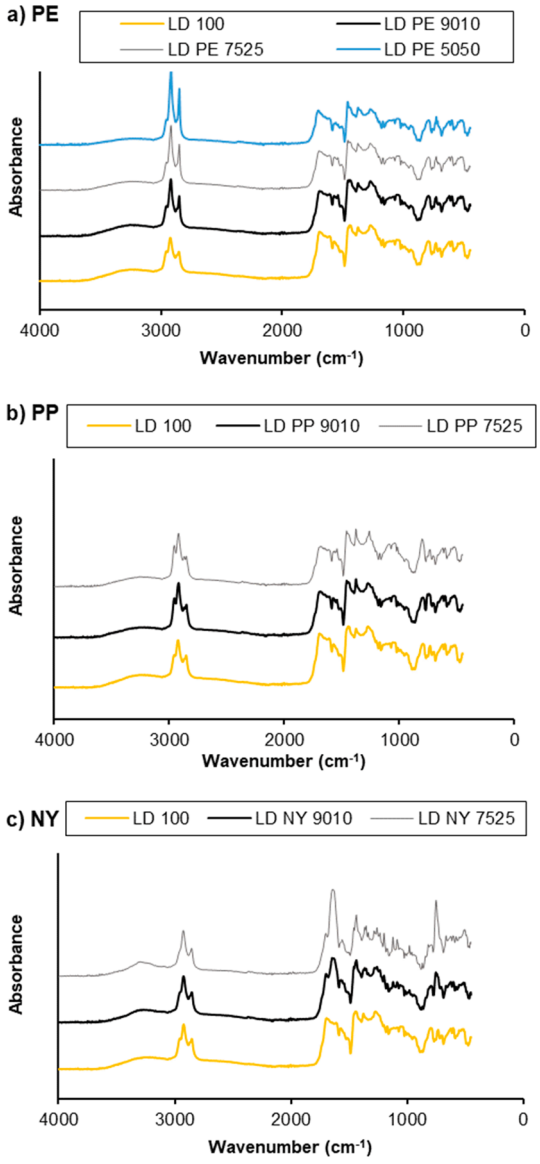

Figure 5. FT-IR spectra of biocrudes obtained from liquefaction of pure *L. digitata* and *L. digitata* blends with PE, PP, and NY.

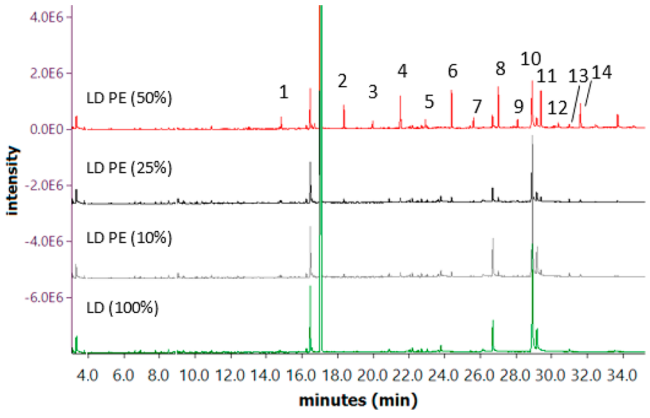

Figure 6. Overlay of GC chromatograms of biocrudes created from *L. digitata*/PE feedstocks at PE blend levels of 0, 10, 25, and 50%. The high-intensity peak at 17.09 min is of solvent origin

Table 2. Identities of Notable Compounds in Biocrude Products from Co-liquefaction of *L. digitata* with PE

peak	RT	compound
1	14.82	2-dodecanone
2	18.35	2-tetradecanone
3	19.96	heptadecane
4	21.52	2-hexadecanone
5	22.92	nonadecane
6	24.39	2-octadecanone
7	25.63	hexadecane
8	27.01	2-nonadecanone
9	28.10	octadecane
10	28.90	octadecenamide
11	29.41	2-docosanone
12	30.37	octadecane
13	30.99	bis(2-ethylhexyl)phthalate
14	31.62	2-pentacosanone

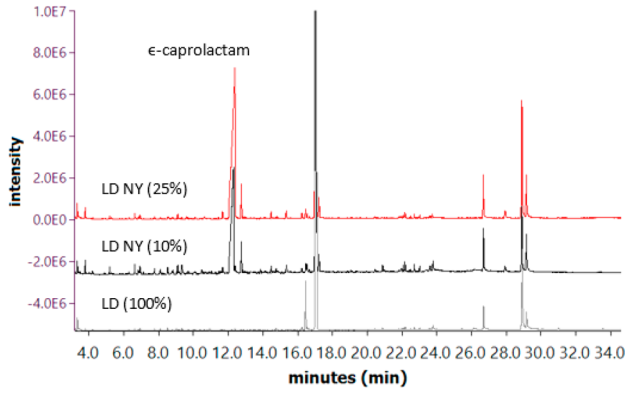

Figure 7. Overlay of GC chromatograms of biocrudes created from *L. digitata*/NY feedstocks at nylon blend levels of 0, 10, and 25%. The high-intensity peak at 17.09 min is of solvent origin.

the presence of NY include tropinone and 2-piperidinemethanol at low levels. The presence of substantial levels of caprolactam in biocrudes and aqueous phase products may present an opportunity for value-addition within the biorefinery.

Aqueous Phase Products. Co-liquefaction of *L. digitata* with PE and PP led to an overall reduction in aqueous phase carbon content. Although the majority of the PE and PP decomposition products were not expected to be water-soluble, the presence of plastics also appears to drive partitioning of biogenic material away from the aqueous phase (Figure 8). In contrast, co-liquefaction with NY increases both the carbon and nitrogen recovered in the aqueous phase materials, predominantly due to the formation of water-soluble caprolactam, which is also present in the oil phase products.

Gas Phase Products. The effect of incorporating plastics into the HTL feedstock on the gas phase products was assessed using GC−MS. The total volumes of the gas phase were only modestly affected in most cases. For the liquefaction of 75:25 blends of *L. digitata* with PE, PP, and NY, the gas phase was composed of 96 wt % CO_2. PE is a highly thermally stable polymer, and thermal degradation tends to result in fragmentation into shorter olefinic fragments via a random scission mechanism, and although monomer production tends to be low,[44] co-liquefaction with PE led to a modest increase in

DOI: 10.1021/acssuschemeng.8b06031
ACS Sustainable Chem. Eng. 2019, 7, 6769−6781

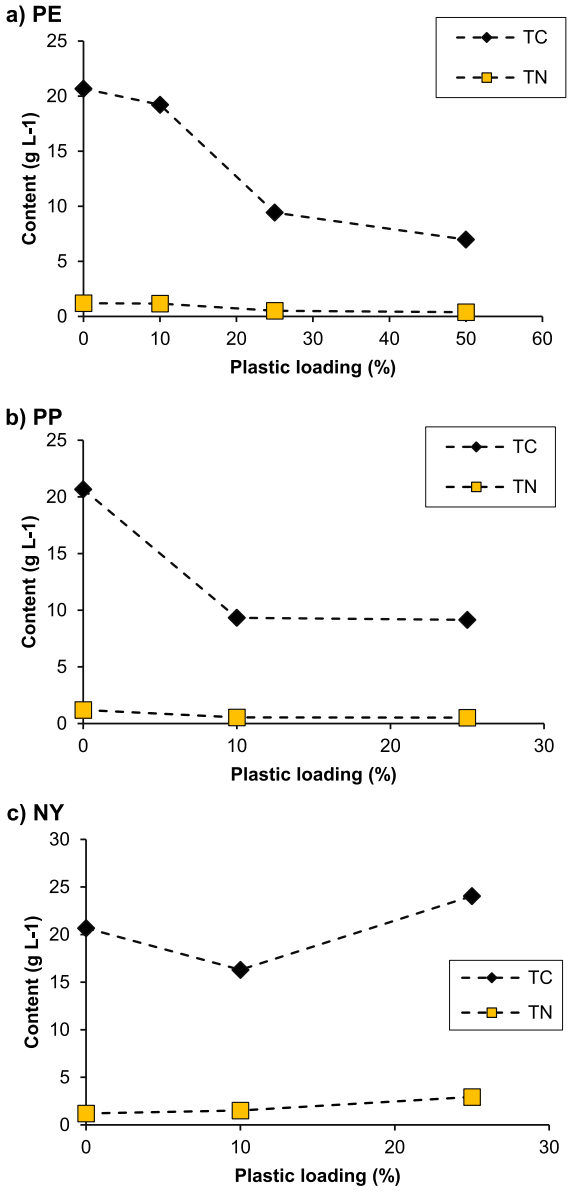

Figure 8. Elemental composition of aqueous phases produced from liquefaction of *L. digitata* blended with (a) PE, (b) PP, and (c) NY.

the production of ethene, as well as ethane, propene, propane, and 1,2-dimethylcyclopropane. For co-liquefaction with PP, a modest increase in the production of propane was observed. In addition to undergoing scission to olefinic fragments of varying sizes,[52] PP can be thermally depolymerized to its monomeric form via a radical mechanism,[44] giving rise to propylene fragments. This radical depolymerization may be accelerated by the presence of biomass ash. An increase in the production of acetaldehyde and acetone was also observed. Somewhat surprisingly, co-liquefaction of *L. digitata* with NY did not appear to contribute to an increase in volatile nitrogenous species. A table of gas phase product compositions may be found in the Supporting Information.

Conversion of Marine Plastics. SEs on biocrude production were evident, but it was unclear to what extent the plastic reacted, and how it was partitioned between the product phases. To determine the amount of plastic-derived (^{14}C-free) carbon in the biocrude, the ^{14}C content was determined by accelerator mass spectrometry (Figure 9). A

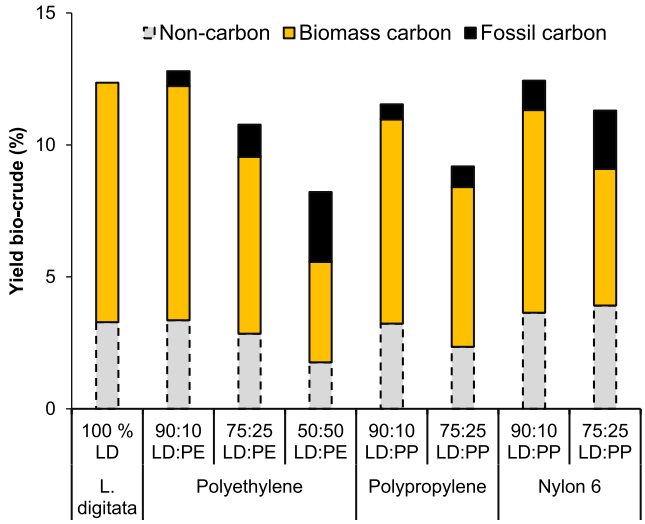

Figure 9. Distribution of biogenic carbon, fossil (plastic) carbon, and other elements in biocrude oils produced from co-liquefaction of *L. digitata* with plastics.

simple two-phase mixing model was employed based on plastic-derived C containing no ^{14}C and using 100% LD biocrude as the biomass C endmember. With increasing plastic blends, an increasing level of fossil carbon (originating from plastics) partitioned to the biocrude products. For PE, approximately 7% of the total carbon in the plastic feedstock was converted to biocrude products at each blend level, constituting up to 41% of the total biocrude carbon content for a 50% blend.

For PP, 7% of the plastic carbon was converted to biocrude products at a 10% blend level, although this decreased to only 4% conversion at a 25% blend. In each case, the presence of biomass facilitated the conversion of plastic to biocrude products, but the presence of plastic caused a modest decrease in the conversion of biomass. For both PP and PE, low levels of volatiles were observed in the gas phase products, while aqueous phase carbon levels were depleted with decreasing biomass in the feedstock. It therefore seems likely that any reacted plastics either partitioned to the biocrude or were converted to solid char, while the remaining unreacted plastics also partitioned to the solid phase (Table 3).

Though it is difficult to quantify exactly what proportion of the alkane polymers reacted under HTL conditions, TGA of the solid phase is indicative. A degradation peak observed at around 400 °C is present for the solid phase from the HTL of pure *L. digitata*, but the rate of degradation for pure PE is substantially higher (Figure 10). For the solid phase samples from the macroalgae/plastic blended feeds, the rate of

Table 3. Distribution of Carbon from the Initial Plastic into the Biocrude Phase

plastic	initial plastic loading (wt%)	plastic C partitioning to biocrude (%)
PE	10	7.7
PE	25	6.7
PE	50	7.3
PP	10	6.8
PP	25	3.7
NY	10	18.0
NY	25	14.2

DOI: 10.1021/acssuschemeng.8b06031
ACS Sustainable Chem. Eng. 2019, 7, 6769−6781

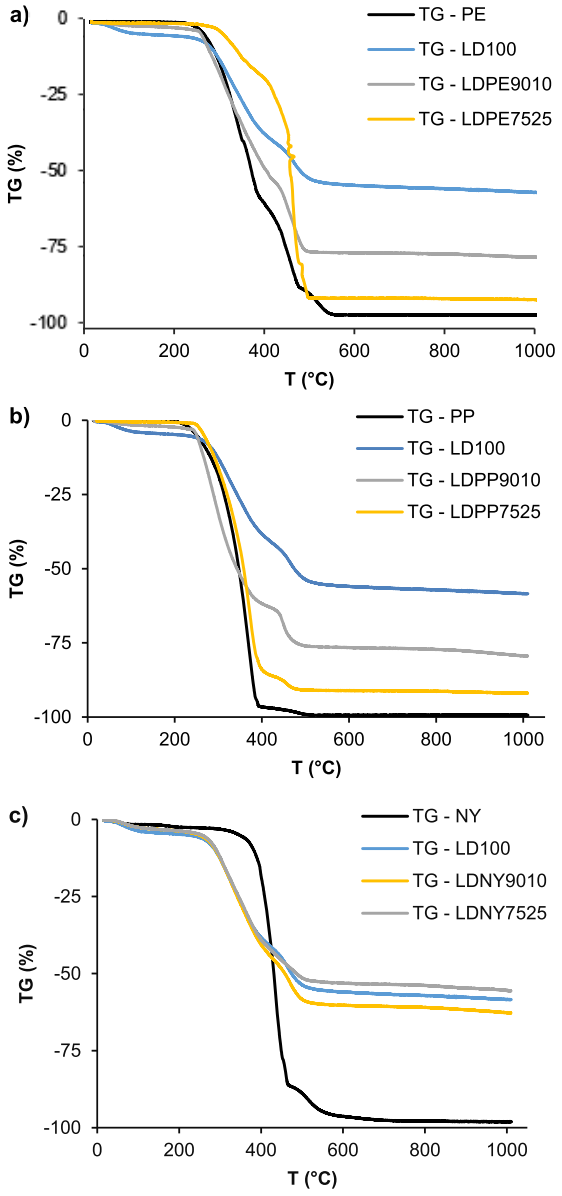

Figure 10. TGA of pure plastics and solid phase products from co-liquefaction of *L. digitata* with plastics.

degradation increases progressively with increasing plastic blend, suggesting that there is a substantial quantity of unreacted PE in the solids. For PP, almost no degradation is seen within the 400−500 °C range, unlike for the solid phase from the HTL of *L. digitata*. With increasing PP blend levels, degradation between 400 and 500 °C becomes less pronounced, suggesting that unreacted PP is present. This suggests that while more of the polymers break down under HTL conditions with macroalgae present, a significant proportion of the plastic retains some of its macrostructure and remains in the solid phase.

However, for NY, the TGA profiles of the solid phases from the liquefaction of *L. digitata* alone and with 10 and 25% blends are almost identical, and markedly different to the TGA curve for pure NY. This indicates that, although some carbon of fossil origin does indeed partition to the solid phase products for NY co-liquefaction, it is highly unlikely to be in the form of unreacted polymeric or oligomeric species but has instead been incorporated into the solid phase products in the form of new molecules.

The caprolactam depolymerization product is soluble in both aqueous and biocrude phases, and a large increase in TC in the aqueous phase is observed upon increasing nylon content in the feed. At both 10 and 25% NY blend levels, approximately 14% of the total fossil carbon was found to have partitioned to the solid phase; whereas 18% of the fossil carbon partitioned to the biocrude phase at the 10% blend level, decreasing to 14% at a 25% blend level. In both cases, 13−14% of the NY carbon partitioned to the solid phase, with 68 and 73% remaining dissolved in the aqueous phase products (Figure 11).

Hydrocarbon contaminants found in harvested marine biomass will likely partition into the solid phase on HTL processing, with minimal conversion into biocrude, but waste biomass rich in NY (commonly originating from fishing line and nets) presents a promising source of value through the recovery of caprolactam from the aqueous phase.

Co-liquefaction of Alternative Macroalgal Species with Plastics. Having examined the effect of coprocessing of *L. digitata* with plastics in detail, co-liquefaction of PE, PP, and NY was also carried out with the brown macroalgae *Fucus serratus* and *Sargassum muticum* and the green macroalga *Ulva lactuca* (Figure 12).

In general, on the addition of PE, overall mass yields of biocrude tended to decrease or stay approximately constant. A modest increase in yield was observed for a 10% blend of PE with *S. muticum*, while decreases in overall biocrude production were observed for 25% blends of PE with all three feedstocks. The majority of the PE was recovered in the solid phase products, with char yields increasing concomitantly with biocrude depletion. Aqueous phase product recovery declined for *F. serratus* and *U. lactuca*, although a modest increase in aqueous phase products was observed for both 10 and 25% blends of PE with *S. muticum*. For all three macroalgae, increasing PE blend levels also caused a modest increase in the yield of gas phase products.

A similar pattern of results was observed for PP. Biocrude yields stayed constant for 10% blends of PP with *F. serratus* and *U. lactuca* and were depleted relative to liquefaction of pure biomass in all other cases. Total biocrude yields were also depleted for 25% blends of PP.

For co-liquefaction with NY, however, both 10 and 25% blend levels led to an increase in biocrude production relative to pure biomass, although the increase in biocrude yield was not linear. An initial increase from 7.8 to 10.3% biocrude for a

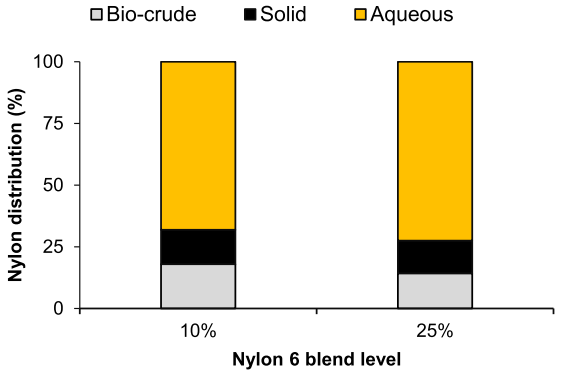

Figure 11. Distribution of NY between HTL product phases.

DOI: 10.1021/acssuschemeng.8b06031
ACS Sustainable Chem. Eng. 2019, 7, 6769−6781

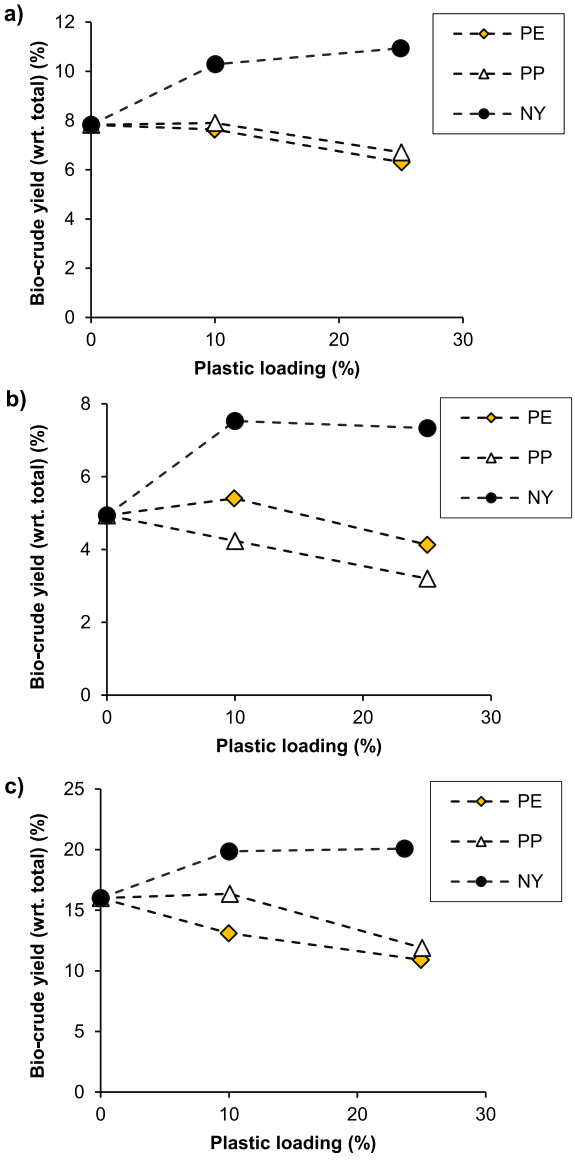

Figure 12. Biocrude yields from liquefaction of blended macroalgae/plastic feedstocks, (a) *F. serratus*, (b) *S. muticum*, and (c) *U. lactuca* (PE = polyethylene, PP = polypropylene, and NY = nylon-6).

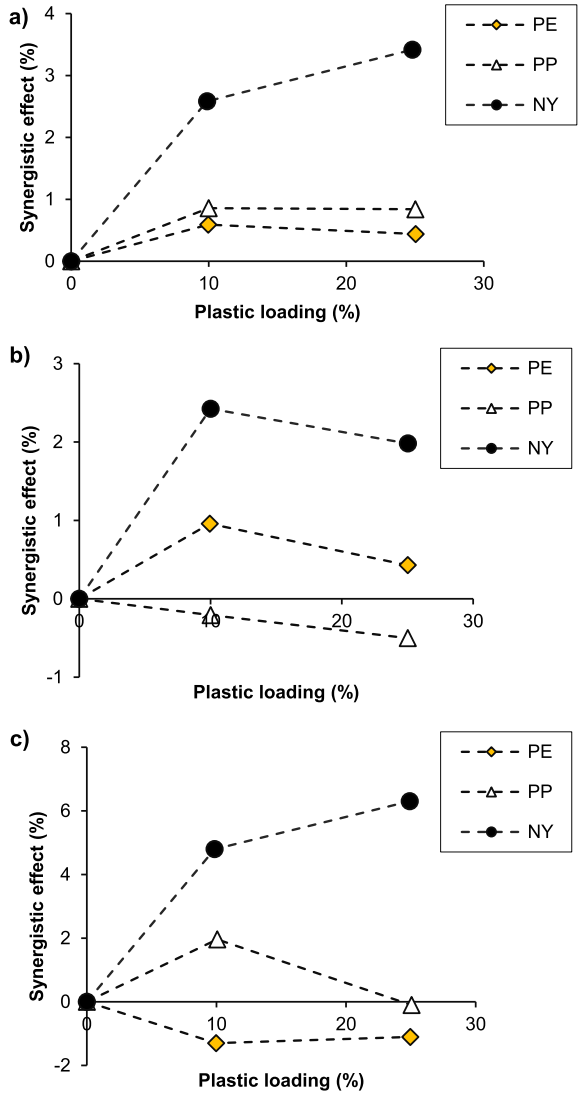

Figure 13. SEs on biocrude yields from liquefaction of blended macroalgae/plastic feedstocks, (a) *F. serratus*, (b) *S. muticum*, and (c) *U. lactuca* (PE = polyethylene, PP = polypropylene, and NY = nylon 6).

10% blend of *F. serratus* with NY was only boosted to 10.9% at the 25% blend level. Similar effects were observed for *U. lactuca* (an initial increase from 16.0 to 19.9%, followed by a modest biocrude yield increase to 20.1%); whereas, for *S. muticum*, yields of 4.9, 7.5, and 7.3% were observed for pure biomass and 10 and 25% PP blend levels, respectively.

The SEs of coprocessing are presented in Figure 13; full product mass balances are presented in the Supporting Information. The degree of SEs for co-liquefaction of each of the three macroalgae species with PE and PP was variable but, for the most part, relatively modest, limited to ±1%. Positive SEs were observed for the co-liquefaction of PE with *F. serratus* and *S. muticum*, while a detrimental effect was observed for *U. lactuca*. For PP, positive SEs on biocrude production were observed for *F. serratus* and *U. lactuca* but not for *S. muticum*. However, for NY, SEs were strongly positive in all instances, with a maximum SE of 7.9% for a 1:3 blend of *U. lactuca* with nylon.

The disparity in SEs observed for the four macroalgae species examined are likely to arise from variation in biomass composition. Different types and levels of proteins, lipids, and carbohydrates may be capable of generating different types of radicals capable of promoting plastic depolymerization. Ash content and composition, in particular, may play a role in determining the degree of plastic conversion; different metals may catalyze or inhibit plastic depolymerization or secondary reactions with biomass decomposition products. The biochemical compositions of *L. digitata*, *F. serratus*, *S. muticum*, and *U. lactuca* are presented in Table 4.

The most pronounced difference in biocrude production between the four species analyzed is the substantially stronger interactions between *U. lactuca* and NY, especially compared to *L. digitata*. This could potentially be explained by the elevated ash content of *U. lactuca* relative to the other macroalgae tested and the comparatively depleted ash content of *L. digitata*. The depolymerization of nylons can be catalyzed by strong mineral acids, strong bases, and some oxides and salts of transition metals, including Zn, Co(II), Cu(II),

DOI: 10.1021/acssuschemeng.8b06031
ACS Sustainable Chem. Eng. 2019, 7, 6769−6781

Table 4. Biochemical Compositions of Macroalgae Coprocessed with Plastics

species	carbohydrate[a] (%)	lipid (saturated) (%)	lipid (unsaturated) (%)	protein (%)	ash (%)
L. digitata	71.6	0.52	0.78	8.58	18.23
F. serratus	63.1	1.09	1.34	11.23	22.72
S. muticum	65.1	0.66	0.53	8.7	24.61
U. lactuca	63.5	0.82	0.33	6.81	27.84

[a]Calculated by difference.

Mn(II), and Cr(III) chlorides, as well as $Mg(OH)_2$.[53] Macroalgal ash contains a wide range of metals, the composition of which varies depending on the metals present in the marine environment, but macroalgae of the genus *Ulva* are considered to be good metal bioaccumulators and are often used as indicators of aqueous metal pollution.[54] It is likely that *U. lactuca* contained higher levels of catalytic transition metal species, which activated nylon depolymerization, while the content of the relevant metals in *L. digitata* may have been lower. A detailed analysis of the exact metals present in the ash would be beneficial in further elucidation of the reaction mechanisms.

The strongest SEs in terms of PE conversion were observed for *L. digitata*. PE decomposition is speculated to occur via a radical mechanism, and it is, therefore, possible that *L. digitata* contains compounds more prone to radical formation. For instance, polyunsaturated lipids are more susceptible to radical peroxidation[55] and could contribute to a higher concentration of radicals within the reaction mixture, which could, in turn, promote the decomposition of PE. Although *F. serratus* contains higher levels of unsaturated lipids than *L. digitata* and exhibits comparatively low activity SEs with respect to PE, the concurrent action of multiple radical formation mechanisms within *L. digitata* could serve to enhance its activity toward PE. Ultimately, the interplay between the many hundreds of individual reactions occurring under HTL conditions between biomass and plastics is complex and merits further study.

CONCLUSIONS

Plastic pollution is ubiquitous throughout the marine environment. Any large-scale industrial biorefinery process exploiting marine biomasses will therefore be exposed to fluctuating quantities of plastic of diverse composition. In this study, the effect of common marine plastic pollutants on HTL of four UK macroalgae species was assessed. PE, PP, and NY were found to interact with biomass under HTL conditions; plastic reactivity in subcritical water was enhanced by the presence of reactive biomass fragments; and rather than inhibiting the process, SEs were observed. The presence of plastics in macroalgal HTL feedstocks led to compositional changes in the resulting biocrudes, giving an overall improvement in biocrude fuel properties for PE and PP but a decrease in total energy content and an increase in nitrogen for NY. PE, unreactive under HTL conditions in isolation, was found to partially fragment into long-chain hydrocarbons and undergo oxidative depolymerization to contribute long-chain ketones to the biocrude products when processed alongside biomass, though less than 10% of the polymer was deposited into this phase. Alternatively, NY almost entirely depolymerized to monomeric caprolactam. Coprocessing of plastics alongside marine biomass can serve the purpose of improving biocrude energy content, but the presence of heteroatoms, such as nitrogen in nylon, may necessitate additional steps in biocrude preprocessing prior to utilization as a fuel. Considering the simplicity of nylon depolymerization, separation of nylon-based marine litter for regeneration of caprolactam may present an additional lucrative revenue stream. Rather than being regarded as problematic contaminants of marine-derived biomasses to be tolerated reluctantly in a biorefinery setting, plastics represent an interesting opportunity to further improve on the process economics. Indeed, the controlled addition of waste plastics to farmed or opportunistically harvested macroalgal biomasses prior to their conversion via HTL may ultimately prove to be a useful tool in dealing with the plastic problem blighting the 21st century.

ASSOCIATED CONTENT

Supporting Information

The Supporting Information is available free of charge on the ACS Publications website at DOI: 10.1021/acssuschemeng.8b06031.

Composition of gas phase products, identities of compounds, batch set-up, heating and cooling profiles, full mass balance, proposed radical mechanism, and mass balances (PDF)

AUTHOR INFORMATION

Corresponding Authors

*E-mail: mija@pml.ac.uk.
*E-mail: c.chuck@bath.ac.uk.

ORCID

Timothy D. J. Knowles: 0000-0003-4871-5542
Christopher J. Chuck: 0000-0003-0804-6751

Author Contributions

S.R. completed the majority of the laboratory work and writing; T.K. undertook the ^{14}C testing; M.A. and C.C. conceived the study, received the funding, and proofed the final manuscript.

Notes

The authors declare no competing financial interest.

ACKNOWLEDGMENTS

The project has been partially supported by the EPSRC through the Centre for Doctoral Training in Sustainable Chemical Technologies (EP/L016354/1) and by the Rodden-berry Foundation Catalyst Fund grant "SeaClean" awarded to the corresponding authors. Many thanks to Isobel Cole, Tracey Beacham, and Andrew Landels for providing the biochemical analysis of the four macroalgae and to Rosie Allen and Archie Allen for helping to source the seaweed biomass.

REFERENCES

(1) Ross, A.; Jones, J.; Kubacki, M.; Bridgeman, T. Classification of Macroalgae as Fuel and Its Thermochemical Behaviour. *Bioresour. Technol.* **2008**, *99* (14), 6494−6504.

DOI: 10.1021/acssuschemeng.8b06031
ACS Sustainable Chem. Eng. 2019, 7, 6769−6781

(2) Kumar, K.; Ghosh, S.; Angelidaki, I.; Holdt, S. L.; Karakashev, B.; Morales, M. A.; Das, D. Recent Developments on Biofuels Production from Microalgae and Macroalgae. *Renewable Sustainable Energy Rev.* **2016**, *65*, 235−249.
(3) Biller, P.; Ross, A. B. Hydrothermal Processing of Algal Biomass for the Production of Biofuels and Chemicals. *Biofuels* **2012**, *3* (5), 603−623.
(4) Lehahn, Y.; Ingle, K. N.; Golberg, A. Global Potential of Offshore and Shallow Waters Macroalgal Biorefineries to Provide for Food, Chemicals and Energy: Feasibility and Sustainability. *Algal Res.* **2016**, *17*, 150−160.
(5) Stévant, P.; Rebours, C.; Chapman, A. Seaweed Aquaculture in Norway: Recent Industrial Developments and Future Perspectives. *Aquacult. Int.* **2017**, *25*, 1373−1390.
(6) Watson, L.; O'Mahony, F.; Edwards, M.; Dring, M. L.; Werner, A. *The Economics of Seaweed Aquaculture in Ireland Laminaria Digitata and Palmaria Palmata*; Prague, Czech Republic, 2012.
(7) Thomas, J.-B. E.; Nordström, J.; Risén, E.; Malmström, M. E.; Gröndahl, F. The Perception of Aquaculture on the Swedish West Coast. *Ambio* **2017**, *47*, 398−409.
(8) Rebours, C.; Marinho Soriano, E.; Zertuche González, J. A.; Hayashi, L.; Vásquez, J. A.; Kradolfer, P.; Soriano, G.; Ugarte, R.; Abreu, M. H.; Bay Larsen, I.; et al. Seaweeds: An Opportunity for Wealth and Sustainable Livelihood for Coastal Communities. *J. Appl. Phycol.* **2014**, *26*, 1939−1951.
(9) Troell, M.; Halling, C.; Nilsson, A.; Buschmann, A. H.; Kautsky, N.; Kautsky, L. Integrated Marine Cultivation of Gracilaria Chilensis (Gracilariales, Rhodophyta) and Salmon Cages for Reduced Environmental Impact and Increased Economic Output. *Aquaculture* **1997**, *156* (1−2), 45−61.
(10) Nelson, S. G.; Glenn, E. P.; Conn, J.; Moore, D.; Walsh, T.; Akutagawa, M. Cultivation of Gracilaria Parvispora (Rhodophyta) in Shrimp-Farm Effluent Ditches and Floating Cages in Hawaii: A Two-Phase Polyculture System. *Aquaculture* **2001**, *193* (3−4), 239−248.
(11) Broch, O. J.; Ellingsen, I. H.; Forbord, S.; Wang, X.; Volent, Z.; Alver, M. O.; Handå, A.; Andresen, K.; Slagstad, D.; Reitan, K. I.; Olsen, Y.; Skjermo, J. Modelling the Cultivation and Bioremediation Potential of the Kelp Saccharina Latissima in Close Proximity to an Exposed Salmon Farm in Norway. *Aquac. Environ. Interact.* **2013**, *4*, 187−206.
(12) Chopin, T.; Yarish, C.; Wilkes, R.; Belyea, E.; Lu, S.; Mathieson, A.-T. Developing Porphyra/Salmon Integrated Aquaculture for Bioremediation and Diversification of the Aquaculture Industry. *J. Appl. Phycol.* **1999**, *11*, 463−472.
(13) Sanderson, J. C.; Dring, M. J.; Davidson, K.; Kelly, M. S. Culture, Yield and Bioremediation Potential of Palmaria Palmata (Linnaeus) Weber & Mohr and Saccharina Latissima (Linnaeus) C.E. Lane, C. Mayes, Druehl & G.W. Saunders Adjacent to Fish Farm Cages in Northwest Scotland. *Aquaculture* **2012**, *354*−*355*, 128−135.
(14) Buschmann, A. H.; Varela, D. A.; Hernández-González, M. C.; Huovinen, P. Opportunities and Challenges for the Development of an Integrated Seaweed-Based Aquaculture Activity in Chile: Determining the Physiological Capabilities of Macrocystis and Gracilaria as Biofilters. *J. Appl. Phycol.* **2008**, *20*, 571.
(15) Koelmans, A. A.; Gouin, T.; Thompson, R.; Wallace, N.; Arthur, C. Plastics in the Marine Environment. *Environ. Toxicol. Chem.* **2014**, *33* (1), 5−10.
(16) Bruton, T.; Lyons, H.; Lerat, Y.; Stanley, M.; Rasmussen, M. B. A Review of the Potential of Marine Algae as a Source of Biofuel in Ireland (report prepared for Sustainable Energy Ireland) http://www.seai.ie/Publications/Renewables_Publications_/Bioenergy/Algaereport.pdf (accessed Jan 1, 2016).
(17) Ghadiryanfar, M.; Rosentrater, K. A.; Keyhani, A.; Omid, M. A Review of Macroalgae Production, with Potential Applications in Biofuels and Bioenergy. *Renewable Sustainable Energy Rev.* **2016**, *54*, 473−481.
(18) Possatto, F. E.; Barletta, M.; Costa, M. F.; Ivar Do Sul, J. A.; Dantas, D. V. Plastic Debris Ingestion by Marine Catfish: An Unexpected Fisheries Impact. *Mar. Pollut. Bull.* **2011**, *62*, 1098−1102.
(19) Eriksen, M.; Lebreton, L. C. M.; Carson, H. S.; Thiel, M.; Moore, C. J.; Borerro, J. C.; Galgani, F.; Ryan, P. G.; Reisser, J. Plastic Pollution in the World's Oceans: More than 5 Trillion Plastic Pieces Weighing over 250,000 Tons Afloat at Sea. *PLoS One* **2014**, *9* (12), e111913.
(20) Claessens, M.; De Meester, S.; Van Landuyt, L.; De Clerck, K.; Janssen, C. R. Occurrence and Distribution of Microplastics in Marine Sediments along the Belgian Coast. *Mar. Pollut. Bull.* **2011**, *62*, 2199−2204.
(21) Gutow, L.; Eckerlebe, A.; Gimenez, L.; Saborowski, R. Experimental Evaluation of Seaweeds as a Vector for Microplastics into Marine Food Webs. *Environ. Sci. Technol.* **2016**, *50*, 915−923.
(22) *Marine Anthropogenic Litter*; Bergmann, M., Gutow, L., Klages, M., Eds.; Springer International Publishing, 2015.
(23) Kositkanawuth, K.; Bhatt, A.; Sattler, M.; Dennis, B. Renewable Energy from Waste: Investigation of Co-Pyrolysis between Sargassum Macroalgae and Polystyrene. *Energy Fuels* **2017**, *31*, 5088−5096.
(24) Wu, X.; Wu, Y.; Wu, K.; Chen, Y.; Hu, H.; Yang, M. Study on Pyrolytic Kinetics and Behavior: The Co-Pyrolysis of Microalgae and Polypropylene. *Bioresour. Technol.* **2015**, *192*, 522−528.
(25) Yuan, X.; Cao, H.; Li, H.; Zeng, G.; Tong, J.; Wang, L. Quantitative and Qualitative Analysis of Products Formed during Co-Liquefaction of Biomass and Synthetic Polymer Mixtures in Sub- and Supercritical Water. *Fuel Process. Technol.* **2009**, *90* (3), 428−434.
(26) Wu, X.; Liang, J.; Wu, Y.; Hu, H.; Huang, S.; Wu, K. Co-Liquefaction of Microalgae and Polypropylene in Sub-/Super-Critical Water. *RSC Adv.* **2017**, *7*, 13768.
(27) Pei, X.; Yuan, X.; Zeng, G.; Huang, H.; Wang, J.; Li, H.; Zhu, H. Co-Liquefaction of Microalgae and Synthetic Polymer Mixture in Sub- and Supercritical Ethanol. *Fuel Process. Technol.* **2012**, *93* (1), 35−44.
(28) Coma, M.; Martinez Hernandez, E.; Abeln, F.; Raikova, S.; Donnelly, J.; Arnot, T. C.; Allen, M.; Hong, D. D.; Chuck, C. J. Organic Waste as a Sustainable Feedstock for Platform Chemicals. *Faraday Discuss.* **2017**, *202*, 175−195.
(29) Biller, P.; Ross, A. B. Potential Yields and Properties of Oil from the Hydrothermal Liquefaction of Microalgae with Different Biochemical Content. *Bioresour. Technol.* **2011**, *102* (1), 215−225.
(30) Wagner, J.; Bransgrove, R.; Beacham, T. A.; Allen, M. J.; Meixner, K.; Drosg, B.; Ting, V. P.; Chuck, C. J. Co-Production of Bio-Oil and Propylene through the Hydrothermal Liquefaction of Polyhydroxybutyrate Producing Cyanobacteria. *Bioresour. Technol.* **2016**, *207*, 166−174.
(31) Raikova, S.; Smith-Baedorf, H.; Bransgrove, R.; Barlow, O.; Santomauro, F.; Wagner, J. L.; Allen, M. J.; Bryan, C. G.; Sapsford, D.; Chuck, C. J. Assessing Hydrothermal Liquefaction for the Production of Bio-Oil and Enhanced Metal Recovery from Microalgae Cultivated on Acid Mine Drainage. *Fuel Process. Technol.* **2016**, *142*, 219−227.
(32) Channiwala, S. A. A.; Parikh, P. P. P. A Unified Correlation for Estimating HHV of Solid, Liquid and Gaseous Fuels. *Fuel* **2002**, *81* (8), 1051−1063.
(33) Wacker, L.; Nemec, M.; Bourquin, J. A Revolutionary Graphitisation System: Fully Automated, Compact and Simple. *Nucl. Instrum. Methods Phys. Res., Sect. B* **2010**, *268*, 931−934.
(34) Wacker, L.; Christl, M.; Synal, H.-A. BATS: A New Tool for AMS Data Reduction. *Nucl. Instrum. Methods Phys. Res., Sect. B* **2010**, *268*, 976−979.
(35) Moriya, T.; Enomoto, H. Characteristics of Polyethylene Cracking in Supercritical Water Compared to Thermal Cracking. *Polym. Degrad. Stab.* **1999**, *65*, 373−386.
(36) Watanabe, M.; Hirakoso, H.; Sawamoto, S.; Adschiri, T.; Arai, K. *Polyethylene Conversion in Supercritical Water*; 1998; Vol. *13*.
(37) Bai, F.; Zhu, C.-C.; Liu, Y.; Yuan, P.-Q.; Cheng, Z.-M.; Yuan, W.-K. Co-Pyrolysis of Residual Oil and Polyethylene in Sub- and Supercritical Water. *Fuel Process. Technol.* **2013**, *106*, 267−274.
(38) Iwaya, T.; Sasaki, M.; Goto, M. Kinetic Analysis for Hydrothermal Depolymerization of Nylon 6. *Polym. Degrad. Stab.* **2006**, *91*, 1989−1995.

DOI: 10.1021/acssuschemeng.8b06031
ACS Sustainable Chem. Eng. 2019, 7, 6769−6781

(39) CRC. Physical Constants of Organic Compounds. In *CRC Handbook of Chemistry and Physics (Internet Version 2018)*; Rumble, J. R., Ed.; CRC Press/Taylor & Francis: Boca Raton, FL, 2018.
(40) Shin, H.-S.; Ahn, H.-S.; Jung, D.-G. Determination of Phenolic Antioxidants in Spilled Aviation Fuels by Gas Chromatography-Mass Spectrometry. *Chromatographia* **2003**, *58*, 495−499.
(41) Raikova, S.; Le, C. D.; Beacham, T. A.; Jenkins, R. W.; Allen, M. J.; Chuck, C. J. Towards a Marine Biorefinery through the Hydrothermal Liquefaction of Macroalgae Native to the United Kingdom. *Biomass Bioenergy* **2017**, *107*, 244−253.
(42) Raikova, S.; Olsson, J.; Mayers, J.; Nylund, G.; Albers, E.; Chuck, C. J. Effect of Geographical Location on the Variation in Products Formed from the Hydrothermal Liquefaction of Ulva Intestinalis. *Energy Fuels* **2018**, DOI: 10.1021/acs.energyfuels.8b02374.
(43) Anastasakis, K.; Ross, A. B. Hydrothermal Liquefaction of the Brown Macro-Alga Laminaria Saccharina: Effect of Reaction Conditions on Product Distribution and Composition. *Bioresour. Technol.* **2011**, *102* (7), 4876−4883.
(44) Singh, B.; Sharma, N. Mechanistic Implications of Plastic Degradation. *Polym. Degrad. Stab.* **2008**, *93*, 561−584.
(45) Faeth, J. L.; Valdez, P. J.; Savage, P. E. Fast Hydrothermal Liquefaction of Nannochloropsis Sp. To Produce Biocrude. *Energy Fuels* **2013**, *27* (3), 1391−1398.
(46) Zhang, B.; von Keitz, M.; Valentas, K. Thermal Effects on Hydrothermal Biomass Liquefaction. *Appl. Biochem. Biotechnol.* **2008**, *147* (1), 143−150.
(47) Ojha, D. K.; Vinu, R. Copyrolysis of Lignocellulosic Biomass With Waste Plastics for Resource Recovery. In *Waste Biorefinery: Potential and Perspectives*; Pandey, A., Bhaskar, T., Mohan, S. V., Lee, D.-J., Khanal, S. K., Eds.; Elsevier B.V.: Amsterdam, Netherlands, 2018; p 381.
(48) Wong, S. L.; Ngadi, N.; Amin, N. A. S.; Abdullah, T. A. T.; Inuwa, I. M. Pyrolysis of Low Density Polyethylene Waste in Subcritical Water Optimized by Response Surface Methodology. *Environ. Technol.* **2016**, *37* (2), 245−254.
(49) Arturi, K. R.; Kucheryavskiy, S.; Søgaard, E. G. Performance of Hydrothermal Liquefaction (HTL) of Biomass by Multivariate Data Analysis. *Fuel Process. Technol.* **2016**, *150*, 94−103.
(50) George, P.; Rideal, E. K.; Robertson, A. The Oxidation of Liquid Hydrocarbons. I. The Chain Formation of Hydroperoxides and Their Decomposition. *Source Proc. R. Soc. London. Ser. A, Math. Phys. Sci.* **1946**, *185* (1002), 288−309.
(51) Barkby, C. T.; Lawson, G. Analysis of Migrants from Nylon 6 Packaging Films into Boiling Water. *Food Addit. Contam.* **1993**, *10* (5), 541−553.
(52) Aguado, J.; Serrano, D.; San Miguel, G. European Trends in the Feedstock Recycling of Plastic Wastes. *Glob. NEST J.* **2007**, *9* (1), 12−19.
(53) Levchik, S. V.; Weil, E. D.; Lewin, M. Thermal Decomposition of Aliphatic Nylons. *Polym. Int.* **1999**, *48* (7), 532−557.
(54) Villares, R.; Puente, X.; Carballeira, A. Ulva and Enteromorpha as Indicators of Heavy Metal Pollution. *Hydrobiologia* **2001**, *462*, 221−232.
(55) Hampel, M.; Blasco, J.; Martín Díaz, M. L. *Biomarkers and Effects*; Elsevier, 2016.

DOI: 10.1021/acssuschemeng.8b06031
ACS Sustainable Chem. Eng. 2019, 7, 6769−6781